

Platelet Activating Factor Receptor Activation Improves siRNA Uptake and RNAi Responses in Well-differentiated Airway Epithelia

Sateesh Krishnamurthy¹, Mark A Behlke², Michael A Apicella³, Paul B McCray Jr^{1,4} and Beverly L Davidson^{1,5,6}

Well-differentiated human airway epithelia present formidable barriers to efficient siRNA delivery. We previously reported that treatment of airway epithelia with specific small molecules improves oligonucleotide uptake and facilitates RNAi responses. Here, we exploited the platelet activating factor receptor (PAFR) pathway, utilized by specific bacteria to transcytose into epithelia, as a trigger for internalization of Dicer-substrate siRNAs (DsiRNA). PAFR is a G-protein coupled receptor which can be engaged and activated by phosphorylcholine residues on the lipooligosaccharide (LOS) of nontypeable *Haemophilus influenzae* and the teichoic acid of *Streptococcus pneumoniae* as well as by its natural ligand, platelet activating factor (PAF). When well-differentiated airway epithelia were simultaneously treated with either nontypeable *Haemophilus influenzae* LOS or PAF and transduced with DsiRNA formulated with the peptide transductin, we observed silencing of both endogenous and exogenous targets. PAF receptor antagonists prevented LOS or PAF-assisted DsiRNA silencing, demonstrating that ligand engagement of PAFR is essential for this process. Additionally, PAF-assisted DsiRNA transfection decreased CFTR protein expression and function and reduced exogenous viral protein levels and titer in human airway epithelia. Treatment with spiperone, a small molecule identified using the Connectivity map database to correlate gene expression changes in response to drug treatment with those associated with PAFR stimulation, also induced silencing. These results suggest that the signaling pathway activated by PAFR binding can be manipulated to facilitate siRNA entry and function in difficult to transfect well-differentiated airway epithelial cells.

Molecular Therapy—Nucleic Acids (2014) 3, e175; doi:10.1038/mtna.2014.26; published online 15 July 2014

Subject Category: siRNAs, shRNAs, and miRNAs

Introduction

Small interfering RNA (siRNA) oligonucleotides cannot easily cross cellular membranes because of their size and negative charge. The efficient delivery of siRNA oligonucleotides remains a major challenge for advancing RNA interference (RNAi) technology, particularly to the airway. Although the airways can support direct topical delivery, both extra- and intracellular barriers present obstacles for successful RNAi therapy.^{1,2} While several studies reported therapeutic effects following naked siRNA delivery to the lungs^{3–12} others have suggested alternative off target explanations for the results.^{7,9,13,14} Additional data support these findings; siRNA oligonucleotides enter cell poorly, and as a result are not well retained in the respiratory epithelium.^{15,16}

We also reported earlier that Dicer-substrate siRNA (DsiRNA) formulations failed to silence genes in well-differentiated airway epithelia, irrespective of the dose or time of transfection, and that this lack of efficiency correlated strongly with limited oligonucleotide entry.¹⁷ However, we discovered that pretreatment with certain small molecules, as well as enhancers of macropinocytosis such as epidermal growth factor, improved synthetic oligonucleotide uptake and RNAi responses. This result suggested that mechanisms promoting siRNA oligo internalization into differentiated airway epithelia might facilitate RNAi responses.

In this work, we considered mechanisms that microorganisms exploit to enter cells. Following receptor binding, many viruses and bacteria cross cell membranes by one or more endocytic pathway including phagocytosis, clathrin- or caveolae-mediated endocytosis, or macropinocytosis.^{18,19} An elegant study by Ketterer *et al.*¹⁸ showed that the opportunistic pathogen of the airway, nontypeable *Haemophilus influenzae* (NTHi), entered human bronchial epithelia by macropinocytosis after initiating cytoskeletal rearrangement. Further study by the same group demonstrated that NTHi invaded host cells by first binding to the host receptor platelet activating factor receptor (PAFR) via its lipooligosaccharide (LOS)²⁰ glycoforms containing phosphorylcholine (Chop).^{21,22} The adherence and invasion of another bacterium, *Streptococcus pneumoniae* (pneumococcus) was also linked to PAFR binding,²³ possibly through the ChoP moiety present in the bacterial cell wall. Thus, the bacteria's interaction with PAFR provides for cell entry.

PAFR is a G-protein coupled receptor whose natural ligand is platelet activating factor (PAF), a potent phospholipid which also consists of the ChoP moiety in NTHi and the pneumococcal cell wall. Since PAFR stimulation is involved in bacterial entry,²⁴ we hypothesized that PAFR activation might also facilitate macromolecules entry such as siRNA.

We tested this hypothesis on well-differentiated human airway epithelia (HAE) grown at the air–liquid interface (ALI)

¹Department of Internal Medicine, Carver College of Medicine, University of Iowa, Iowa City, Iowa, USA; ²Integrated DNA Technologies, Inc., Coralville, Iowa, USA; ³Department of Microbiology, Carver College of Medicine, University of Iowa, Iowa City, Iowa, USA; ⁴Department of Pediatrics, Carver College of Medicine, University of Iowa, Iowa City, Iowa, USA; ⁵Department of Neurology, Carver College of Medicine, University of Iowa, Iowa City, Iowa, USA; ⁶Molecular Physiology and Biophysics, Carver College of Medicine, University of Iowa, Iowa City, Iowa, USA. Correspondence: Beverly L Davidson, 5060 Colket Translational Research Building, Children's Hospital of Philadelphia, Philadelphia, Pennsylvania 19104, USA. E-mail: davidsonbl@email.chop.edu
Received 8 February 2014; accepted 9 May 2014; published online 15 July 2014. doi:10.1038/mtna.2014.26

and assessed the ability of DsiRNAs to silence endogenous or exogenous targets with or without PAFR stimulation. We show that DsiRNA transfection in combination with PAFR engagement by any of its cognate binding partners or by small molecule treatment improves DsiRNA uptake with concomitant reductions in target RNA and protein levels.

Results

Transfection of DsiRNA into HAE along with LOS or PAF treatment results in silencing of mRNA levels of target gene

Well-differentiated primary cultures of HAE maintained at the ALI model many aspects of the *in vivo* morphology of the surface epithelium and are a useful system in which to test the efficacy of inhibitory RNAs in the form of DsiRNAs.²⁵

We previously reported that DsiRNA transfection in formulation with various transfection agents failed to achieve RNAi in HAE.¹⁷ To test if DsiRNA entry and RNAi responses in HAE can be improved, we activated PAFR in airway cells using some of its cognate binding partners.

One PAFR ligand is the LOS structure of NTHi. The NTHi LOS contains a highly variable assortment of short polyhexose or lactosamine chains emanating from a tri-heptose-ketodeoxyoctanoate-phosphate-lipid A core region.²⁶ In a form of molecular mimicry, NTHi expresses host carbohydrate structures within the oligosaccharide portion of the LOS, including ChoP. NTHi can adhere to and invade human bronchial epithelial cells via interactions between the ChoP⁺ LOS glycoforms and PAFR.²² We isolated LOS from the native NTHi strains and the three LOS isoforms tested differed in the number of phosphocholine residues and LOS

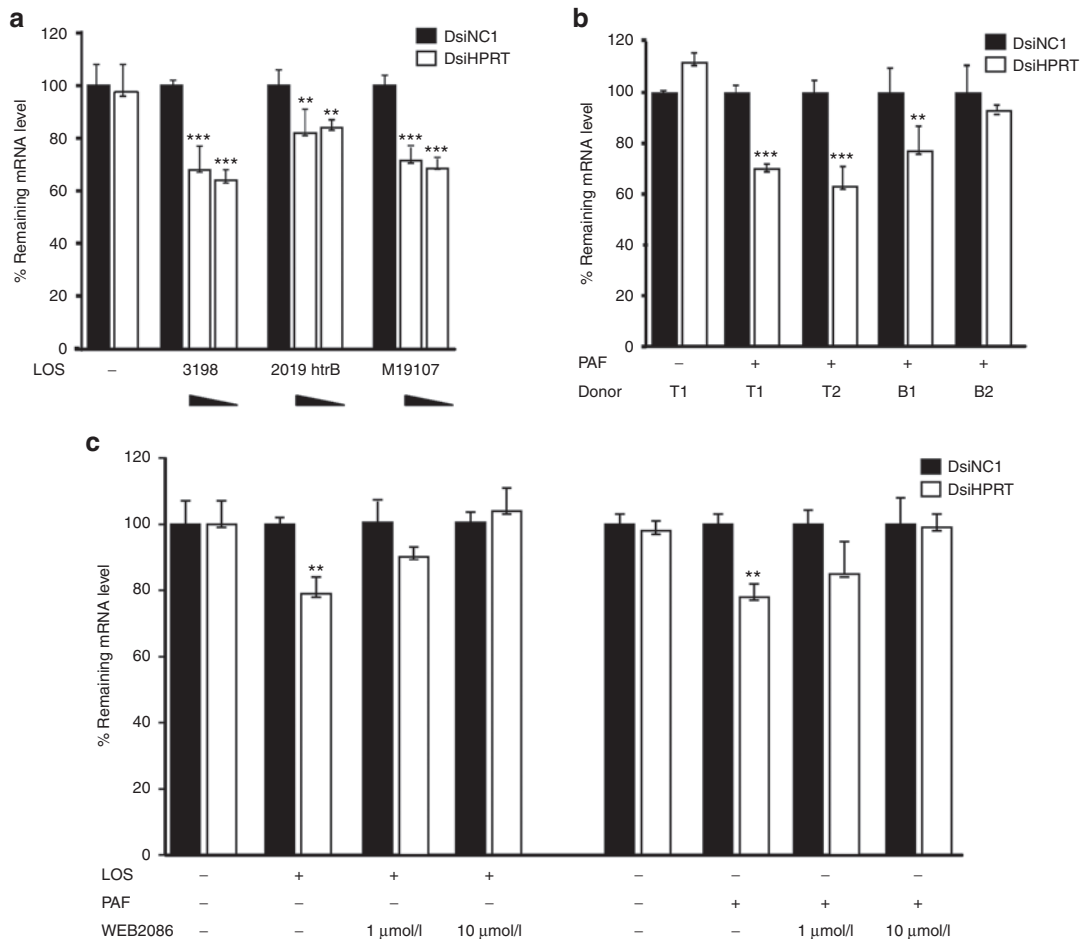


Figure 1 LOS or PAF treatment with simultaneous *HPRT* DsiRNA-Transductin reduces mRNA levels in well-differentiated HAE. **(a)** Well-differentiated HAE cultures grown at the ALI were incubated by adding *HPRT*-targeting or control NC1 DsiRNA (250 nmol/l) formulated with transductin containing 0.1 or 0.01 mg LOS (*HPRT*-targeting DsiRNAs) or 0.1 mg LOS (NC1 DsiRNA; a description of LOS isoforms is provided in **Supplementary Table S1**). After 4 hours, the apical surface was rinsed and 24 hours later, target RNA levels quantified by RT-qPCR. All mRNA levels were normalized to NC1-treated samples. Mean levels were calculated from three biological replicates, each done in triplicate. *** $P < 0.001$, ** $P < 0.01$ (Student's t-test). **(b)** Well-differentiated HAE from four different donors (T1, T1: tracheal epithelial culture; B1, B2: bronchial epithelial culture) were incubated with NC1 and *HPRT* DsiRNA and simultaneously treated with PAF at a concentration of 200 nmol/l for 4 hours, after which the cells were rinsed and mRNA levels determined 24 hrs later. Samples were normalized to NC1-treated cells. *** $P < 0.001$, ** $P < 0.01$ (Student's t-test). **(c)** Well-differentiated HAE were treated with PAFRa (WEB2086) at 1 or 10 $\mu\text{mol/l}$ for 2 hrs, followed by addition of DsiRNAs and transductin (4 hours) with or without PAF (200 nmol/l). PAFRa was present throughout transfection in cells pre-treated with the reagent. Cells were harvested and RNA quantified 24 hrs later. Samples were normalized to NC1-treated cells. ** $P < 0.01$ (Student's t-test).

stability. The details of each LOS isoforms used are provided in **Supplementary Table S1**. When HAE were transduced with a HPRT DsiRNA-transductin formulation and simultaneously treated with each LOS, *HPRT* mRNA levels were reduced by up to 35% when analyzed 24 hours after transduction (**Figure 1a**) compared to negligible transduction in the absence of the LOS.

The natural ligand for PAFR is the potent phospholipid activator, PAF. We hypothesized that PAF activation of PAFR during DsiRNA transduction would improve RNAi responses in HAE as seen with LOS. PAF binding to PAFR activates several signaling mechanisms including GTPase activation causing phospholipid turnover (via phospholipases C, D, and A2 pathways) and protein kinase C and tyrosine kinase activation.²⁷ Epithelia were PAF treated for 4 hours in the presence of the DsiRNA mixture, rinsed, and then incubated for a further 24 hours before gene expression was measured by RT-qPCR. Treatment of HAE with DsiRNA-transductin and PAF reduced *HPRT* mRNA levels between 10 and 40% depending on the donor cell culture (**Figure 1b**). A dose-response relationship for PAF on DsiRNA silencing was observed (**Supplementary Figure S1a**). We also investigated the duration of knock down after PAF-assisted transfection. Following delivery, epithelia were studied on days 1, 3, 6, and 10. *HPRT* mRNA levels were significantly reduced 1 and 3 days post transfection. By 6 and 10 days, the transcript levels were returning to basal levels (**Supplementary Figure S1b**). Since each mRNA target is likely to have a different rate of turnover, repeated transfection may be necessary to maintain knockdown.

A well-studied effect of PAFR stimulation is the activation of mediators that can generate inflammatory responses (38–41). As a mediator of inflammation, PAFR activation can alter tight junction integrity in endothelial and intestinal epithelial cells.^{28,29} We examined the effects of PAF on tight

junction integrity in airway epithelia. PAF application to the apical and basolateral surfaces of HAE for 8 hours caused no alteration of tight junction morphology as assessed by ZO-1 immunostaining. In contrast, 24 hours of PAF treatment caused significant alterations in tight junction morphology (**Supplementary Figure S2a**). Our experimental protocol involved PAF treatment of epithelia during DsiRNA transduction for 4 hours; hence its effects on tight junction should be minimized. We also examined epithelial cell morphology after PAF-assisted transfection. Epithelial sheets were fixed, sectioned, and stained with hematoxylin–eosin (H&E) 1 and 10 days after transfection, and these sheets showed no changes in cell morphology when compared with control treated epithelium (**Supplementary Figure S2b**). Cytotoxicity was also assessed by lactate dehydrogenase release. Both PAF and control treated cells showed minimal evidence of cytotoxicity (**Supplementary Figure S2c**).

The PAFR-dependence of the LOS- and PAF-mediated enhancement of DsiRNA silencing was evaluated using the PAF receptor antagonist (PAFRa) WEB2086. Pre- or post-treatment of epithelia with 100 $\mu\text{mol/l}$ PAFRa completely inhibited *HPRT* silencing of either LOS- or PAF-assisted transduction samples (**Figure 1c**). Lower concentrations of PAFRa (1 $\mu\text{mol/l}$) partially inhibited silencing in cells transduced with LOS or PAF (**Figure 1c**). These results suggest that the effects of LOS and PAF on siRNA-mediated silencing are a consequence of their interactions with PAFR.

PAF treatment enhances DsiRNA entry and uptake into cells

We next asked whether the improved RNAi responses following PAFR stimulation were due to an increase in uptake and internalization of DsiRNA. When digoxigenin (DIG)-labeled DsiRNA was transduced in formulation with transductin in PAF-treated HAE, we observed a substantial increase in the amount of internalized label 1 hour later (**Figure 2b**) compared with control HAE (**Figure 2a**). These data suggests that improved RNAi upon PAFR stimulation is a result of improved DsiRNA internalization.

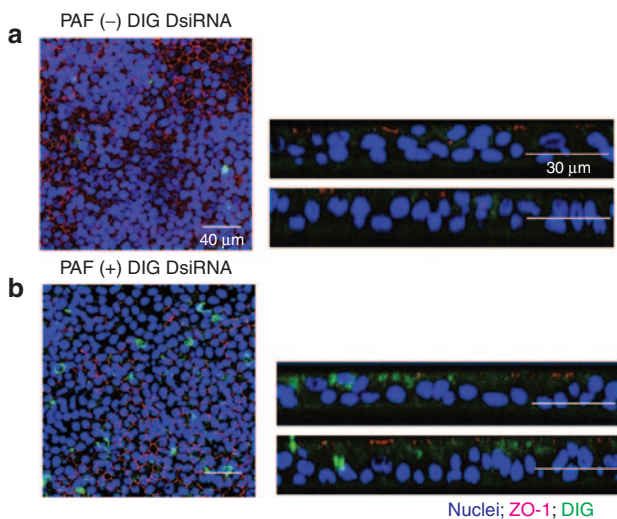


Figure 2 PAF treatment enhances DsiRNA entry and uptake into cells. Confocal images (x-y, left panels; x-z stacks, right panels) of epithelia 1 hour after transduction with DIG-labeled DsiRNA complexed with transductin, (a) without or (b) with PAF treatment (200 nmol/l). Blue, nuclei; green, DIG-labeled oligo; red, ZO-1. The images on the right and the left are from different fields.

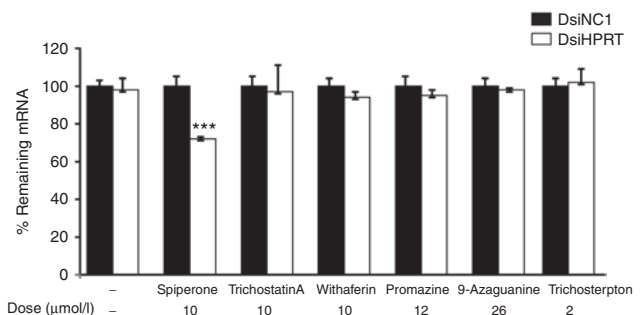


Figure 3 Spiperone improves RNAi responses in DsiRNA transduced cells. HAE were pre-treated with various small molecules at the concentration indicated. The drugs were added to the apical surface and the basolateral media for 6 hours. Both surfaces were then rinsed and *HPRT* or NC1 DsiRNA formulated with transductin added to the apical surface. The cells were rinsed after 4 hours, and RT-qPCR done on cell lysates harvested 24 hours later. Data show *HPRT* mRNA levels normalized to NC1-treated samples (three biological replicates –in triplicate). *** $P < 0.001$ (Student's *t*-test).

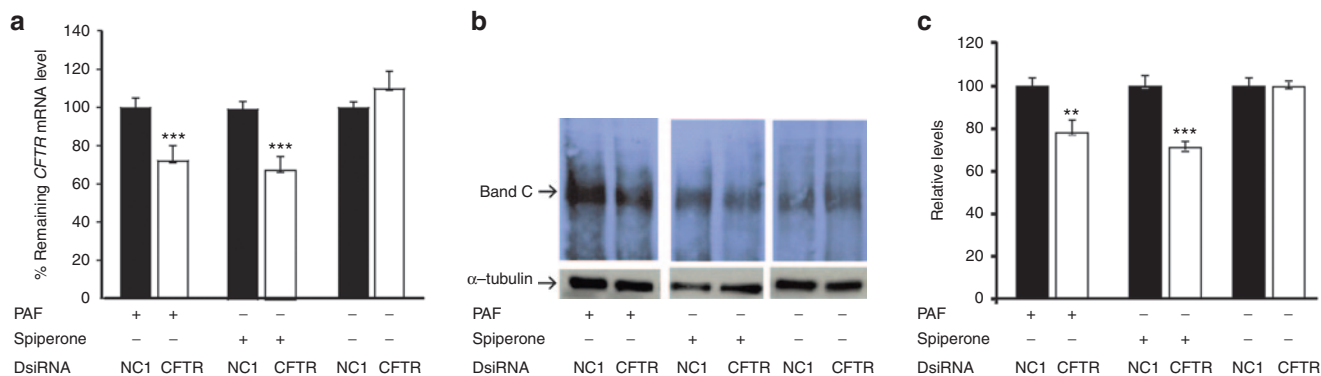


Figure 4 PAF or spiperone treatment decreases CFTR protein levels in HAE treated with CFTR DsiRNA. (a) PAF and DsiRNA (*CFTR*-targeting or control NC1 in transductin), were applied to well-differentiated HAE for 4 hours. Alternatively, spiperone was applied apically and basolaterally to well-differentiated HAE for 6 hours, and then removed by rinsing before incubation for 4 hours with *CFTR*-targeting or NC1 DsiRNAs complexed with transductin. In both cases, 24 hours after transfection, and RNA levels quantified by RT-qPCR. (b) A representative immunoblot from similarly treated wells, but cells were lysed and proteins visualized after immunoprecipitation with anti-CFTR antibody. Alpha-tubulin was used as a loading control. (c) Densitometry readings of immunoblots with results normalized to NC1 treated samples. In all cases, data are from 3 biological replicates and are mean \pm SD. *** $P < 0.001$; ** $P < 0.01$ (Student's *t*-test).

Spiperone treatment induces RNAi responses in HAE

The Connectivity map (CMAP) database is a repository of transcriptional profiles from a number of human cell lines in response to drug treatments.³⁰ We correlated the input signatures of gene expression changes during PAFR activation from a previously published microarray study³¹ with those from the CMAP database. The method of analysis is described in more detail in Materials and Methods. The analysis yielded several drugs that correlated positively with PAF-induced changes in gene expression. We reasoned that treatment of HAE with these candidates might induce gene expression changes similar to those associated with PAFR activation. From these data, six candidates were selected and tested. HAE were pretreated with drugs and then subsequently incubated with *HPRT* targeting DsiRNA-transductin formulations as before. Of these interventions, only spiperone pretreatment was effective. Spiperone, an antipsychotic drug, increases intracellular Ca^{2+} levels through a protein kinase-coupled phospholipase C-dependent pathway and also stimulates calcium-activated chloride channels in polarized HAE cells.³² Of note, PAF also activates the phospholipase C pathway.²⁷ Spiperone treatment of epithelia (10 μ mol/l) before DsiRNA transduction resulted in 25% silencing of *HPRT* mRNA levels (Figure 3). A spiperone dose-response showed marginal increases in silencing with increasing doses (Supplementary Figure S3).

PAF or spiperone treatment decreases CFTR protein levels and function in HAE transduced with CFTR DsiRNA

We next asked whether endogenous gene silencing by DsiRNA, facilitated by PAFR activation, reduces target mRNA and protein levels. Cystic fibrosis transmembrane regulator (CFTR) encodes an anion channel in airway epithelia. Loss of CFTR function, caused by mutations in the *CFTR* gene causes cystic fibrosis, an important chronic disease characterized by progressive pulmonary infection and inflammation. DsiRNA incubation with simultaneous PAF treatment or with spiperone pre-treatment caused ~30% silencing of *CFTR* mRNA levels (Figure 4a). Immunoprecipitation

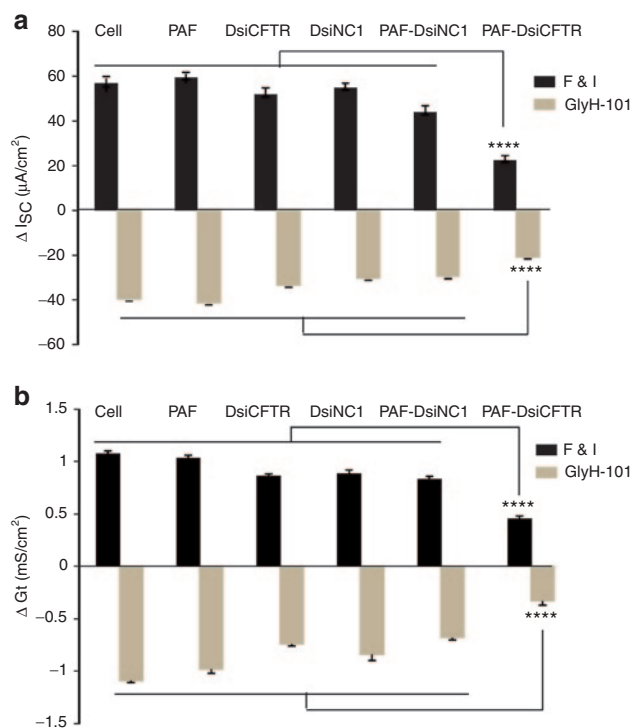


Figure 5 PAF treatment with CFTR DsiRNA reduces CFTR function in HAE. Changes in (a) transepithelial current (ΔI_{sc}) and (b) conductance (ΔG_t) induced by sequential addition of amiloride, Forskolin and IBMX (F&I) and GlyH-101 in HAE cultures treated with the indicated agents. Each bar represents nine replicates from three different donors (three replicates from each). Mean \pm SD. Statistical significance was determined by repeated measures one-way ANOVA **** $P < 0.0001$.

and then western blot analysis in cells treated with PAF or spiperone and *CFTR* DsiRNA-transductin showed reduced CFTR protein levels compared to controls (Figure 4b). Fully glycosylated CFTR band C was significantly decreased in PAF and spiperone-treated cells (Figure 4c). Consequently, well-differentiated airway epithelia allow for

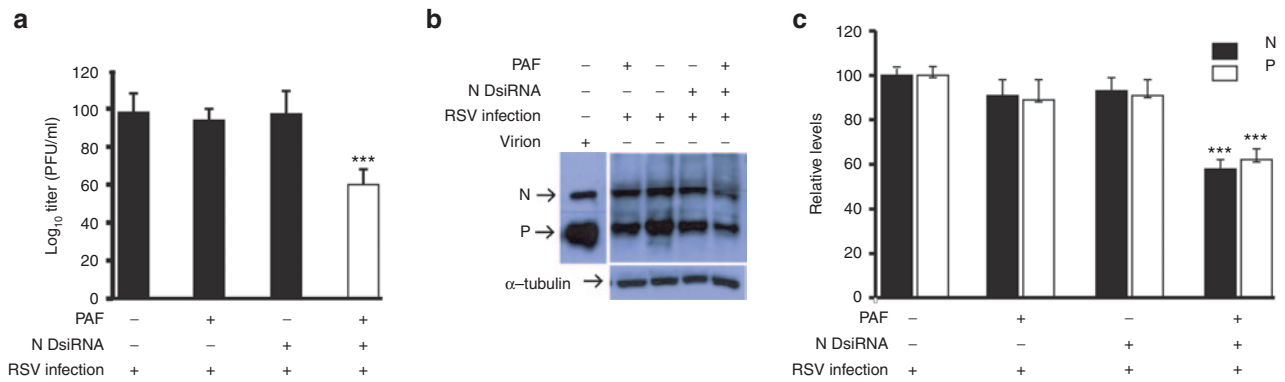


Figure 6 PAF induced DsiRNA uptake reduces RSV protein levels and titer in HAE. HAE was either treated or untreated with PAF in concurrence with RSV N DsiRNA. Six hours later the cells were infected with RSV at an MOI of 1. (a) Forty-eight hours later, the cell washes from the apical surface was collected and assayed for viral titer. The cells were lysed and (b) the proteins visualized after immunoprecipitation with anti-RSV antibodies and (c) the bands quantified by densitometry. Data are mean \pm SD from the results three different experiments, each using a different donor. *** $P < 0.001$ (Student's *t*-test).

silencing of target mRNA and protein when PAFR signaling or PAFR-related gene expression changes are activated.

We next assessed epithelial cell bioelectric properties following PAF-mediated delivery of DsiRNA-transductin targeting *CFTR*; *CFTR* is a phosphorylation and nucleotide activated anion channel that helps regulate the volume and composition of airway surface liquid, and loss of function impairs transepithelial anion transport. In control epithelia with or without PAF treatment (without HPRT DsiRNA transfection) or PAF and scrambled control DsiRNA (NC1) treated cells, the addition forskolin and isobutylmethylxanthine (IBMX) increased the cAMP-activated transepithelial short-circuit current (*I*_{sc} and Δ *I*_{sc}) and conductance (*G*_t and Δ *G*_t) as expected (Supplementary Figure S4; Figure 5a,b). Subsequent addition of GlyH-101, a *CFTR* channel inhibitor, decreased both values. In contrast, PAF treated and *CFTR* DsiRNA-transduced cells showed significantly reduced cAMP-activated changes in transepithelial current and conductance (Supplementary Figure S4; Figure 5a,b). We note that *CFTR* activity is typically not rate-limiting at normal levels of *CFTR* expression. Rather, the activity of transporters/channels at the basolateral membrane limits the magnitude of agonist activated current. Therefore, the magnitude of current reduction observed here may reflect a reduction in *CFTR* protein expression greater than that suggested by current measurements. These results show that PAFR-mediated oligo delivery and *CFTR* knockdown significantly reduced *CFTR* channel activity.

PAF treatment reduces exogenous viral protein with concomitant decrease in titer in DsiRNA transduced HAE

Respiratory Syncytial Virus (RSV) is an important pathogen in children and elderly and immunocompromised individuals. There is neither a preventive vaccine nor an effective treatment for the disease. Potent RNAi against RSV in airway epithelia has not been rigorously demonstrated. Here, we tested the effect of DsiRNA against the RSV *N* gene in infected HAE with or without PAF treatment at the time of oligonucleotide application. Epithelia were PAF treated and incubated with DsiRNA-transductin targeting the *N* gene. Six hours later, the cells were infected with RSV at an MOI of 1. Viral titers calculated from the apical rinses were reduced

more than 100-fold in samples treated with PAF (Figure 6a). PAFR activation alone did not reduce viral titers. Immunoblot analysis 48 hours after infection showed reduced RSV N and P protein abundance compared to untreated control cells (Figure 6b,c). These results demonstrate that PAFR activation enables viral load reduction by facilitating RNAi in airway epithelia.

Discussion

RNAi-based therapeutics has the potential to transform treatments for human diseases. However, there are a number of challenges that must be overcome. One is the efficient delivery to target organs. Local access to the respiratory tract is easily achieved, but barriers including the chemistry of synthetic siRNA oligos and the physical properties of the airways can impede successful delivery. Previous studies^{15–17} and this work illustrate the difficulty in silencing target genes with both naked and vehicle-formulated siRNAs. Cytoplasmic entry and retention of the oligonucleotides essential for further downstream RNAi effects have been shown to be problematic in this target tissue.^{15,17}

Here, we show that PAFR engagement by its natural ligand or a structurally related LOS enhances peptide-mediated DsiRNA uptake and achieves target silencing. By manipulating this pathway for siRNA entry we decreased the abundance of endogenous transcripts and reduced the pathogenic load of an important respiratory virus. Consistent with this result, DsiRNA transfection following spiperone pre-treatment also reduced mRNA transcript abundance.

Different endocytic pathways are used for the uptake of particles or soluble ligands. One mechanism, macropinocytosis, is achieved by plasma membrane ruffling.³³ Macropinocytosis is also a driving force for the entry of some bacteria and viruses.^{19,34,35} Since it is nonselective, there is growing interest in coopting macropinocytosis as a delivery mechanism for macromolecules and therapeutics. The peptide vehicle transductin used in our DsiRNA formulations enters cells via macropinocytosis.^{36,37} We previously observed that transductin facilitated DsiRNA entry and silencing of targets in well-differentiated HAE when combined with enhancers of

macropinocytosis such as EGF^{17,38} or phorbol esters (unpublished data) but could not induce gene silencing when used alone. However, EGF treatment yielded very modest knock-down and phorbol ester, while associated with better silencing, is toxic and unsuitable for repeated applications or use *in vivo*.³⁸ Here, we exploited mechanisms that some respiratory pathogens use for entry. For example, pneumococcus and NTHi adhere to PAFR, which is coupled to the invasion of cells.¹⁸ Additional studies showed that NTHi initiated cytoskeletal rearrangements in HAE resulting in bacterial internalization via macropinocytosis. Studies have also shown that PAF treatment induced endothelial actin cytoskeletal rearrangement.³⁹ Since cellular factors and activation signals are essential requirements for endocytosis, we hypothesized that activating PAFR signaling with known ligands might enhance siRNA internalization and silence target genes. Indeed, we found that PAFR engagement by LOS or PAF was essential for enhanced internalization and silencing of endogenous and exogenous targets.

PAFR is a G-protein coupled receptor that activates several signaling mechanisms after binding to its cognate receptors.⁴⁰ Upon binding, GTPase and phospholipases (C, D, and A2 pathways), protein kinase C (PKC), and tyrosine kinase signaling are activated. Similarly, in human bronchial epithelia, infection with NTHi 2019 increased Ca²⁺ levels and cytosolic inositol phosphate levels²⁷ that were inhibited by a PAF antagonist.²² Spiperone also enhances intracellular Ca²⁺ through a protein-kinase and phospholipase C dependent pathway similar to PAFR activators,³² and when applied to HAE, enhanced silencing. To our knowledge spiperone is the only compound we tested that shares these properties with PAFR activators. Thus, the downstream effects of PAFR activation increase siRNA internalization in airway epithelia.

A potential limitation of this approach is that PAFR signaling also mediates inflammation. PAFR activation in cells and tissues may increase leukocyte trafficking and the generation of inflammatory responses.^{40–43} Related to its induction of actin cytoskeletal rearrangements, PAF-mediated activation of endothelial cells induced vascular permeability and disassembly of interendothelial junctions.²⁸ F-actin and tight junction disruption has also been seen in intestinal epithelial cells.²⁹ We also observed that long-term PAF treatment (greater than 24 hours) reduced tight junction integrity. Although these responses are reversible by PAFR antagonists, such treatment may not be necessary as these exposures are longer than any intended *in vitro* or *in vivo* use. Alternatively, it may be possible to prepare synthetic NTHi LOS that binds PAFR but is noninflammatory. For example pneumococcal interactions with PAF receptor fail to induce proinflammatory signaling cascades.²³ This ability of pneumococci to adhere to PAFR in the absence of signal transduction while retaining the ability to transcytose into cells suggests that uptake of siRNA delivery using this approach could be decoupled from inflammation.

In this work, we noted variability based on the lung donor. To improve on the very modest effects seen in some instances, repetitive dosing may be required. Nonetheless this work demonstrates for the first time that PAFR activation increases siRNA oligo delivery and provides a target

pathway for further implementing the utility of RNAi to treat lung disease or prevent against lung pathogens.

Materials and methods

Culture of primary epithelial cells and cell lines. HAE cells were obtained from trachea and bronchi of lungs removed for organ donation from non-cystic fibrosis individuals. Cells were isolated by enzyme digestion as previously described.⁴⁴ Following enzymatic dispersion, cells were seeded at a density of 5×10^5 cells/cm² onto collagen-coated, 0.6 cm² semi permeable membrane filters (Millipore polycarbonate filters; Millipore, Bedford, MA). The cells were maintained at 37 °C in a humidified atmosphere of 5% CO₂ air. Twenty-four hours after plating, the apical media was removed and the cells were maintained at an ALI to allow differentiation of the epithelium. The culture medium consisted of 1:1 ratio mix of Dulbecco's modified Eagle's medium (DMEM)/Ham's F12, 5% Ultrosor G (Biosepra SA, Cedex, France), 100 U/ml penicillin, 100 µg/ml streptomycin, 1% nonessential amino acids and 0.12 U/ml insulin. Studies were performed on well-differentiated epithelia ~4–6 weeks after initiation of the ALI cultures conditions. HEP-2 cells were maintained in MEM substituted with 10% fetal bovine serum and 100 U/ml penicillin.

DsiRNA oligonucleotides. All oligonucleotides employed in this study were synthesized using standard phosphoramidite chemistry, purified by RP-HPLC and used in sodium salt form IDT (Integrated DNA Technologies, Coralville, IA). The predicted masses for the oligonucleotides were verified by electrospray-ionization mass spectrometry (ESI-MS) and were within $\pm 0.02\%$. The protocol for DsiRNA design and manufacture has been described in detail.^{45,46} The DIG-labeled DsiRNA was made by attaching DIG-NHS ester an internal-dT residue in a 2-O' methyl modified pig-HPRT-specific DsiRNA. The DsiRNAs used in this study are listed in **Supplementary Table S2**.

RNAi transduction. The PTD-DRBD peptide delivery reagent was purchased as Transductin from IDT. Transductin (Integrated DNA Technologies) was developed by Dr Steven Dowdy at the UCSD School of Medicine.⁴⁷ It consists of a small fusion protein comprised of multiple peptide transduction domains connected to a double-stranded RNA binding domain (PTD-DRBD). The fusion protein can be purified from bacteria expressing PTD-DRBD from a modified pTAT vector (available from Dr Dowdy's lab). The detailed protocol for purification of the protein is available.⁴⁷

LOS isolation. LOS was isolated from NTHi strain 3198 or strain 2019htrB⁴⁸ or from *H. hemolyticus* (M19107) using the proteinase K-phenol water method previously described.⁴⁹ Bacteria were grown as a lawn for ~16 hours on brain-heart infusion medium plates with appropriate antibiotics at various temperatures at 37 °C in a CO₂ incubator overnight and were collected by flooding the plates with PBS and scraping colonies from the surfaces. Cells were centrifuged and suspended in a solution of 6 mmol/l Tris base (Research Products International Corporation, Mt. Prospect, IL), 10 mmol/l ethylenediaminetetraacetic

acid (Fisher Scientific, Fair Lawn, NJ), and 2.0% (wt/vol) sodium dodecyl sulfate (SDS) (Research Products International), pH 6.8, containing 50 µg/ml proteinase K, were incubated at 65 °C for 1 hour, and then were incubated overnight at 37 °C. To remove SDS, samples were precipitated with 0.3 mol/l sodium acetate and three volumes cold 100% ethanol, flash cooled in a dry ice-ethanol bath, and incubated overnight at -20 °C. Samples were centrifuged for 10 minutes at 12,000 × g at 4 °C, and pellets were suspended in deionized water and precipitated a total of three times. Samples were suspended in water and treated with 80U micrococcal nuclease (Sigma-Aldrich, St. Louis, MO) for 2 hours at 37 °C. LPS samples and phenol were equilibrated to 65 °C, and an equal volume of phenol was added to the lysates. Samples were mixed, incubated at 65 °C for 30 minutes, cooled on ice, and centrifuged at 3,000 rpm for 10 minutes at 4 °C. The aqueous layer was collected, and the organic layer was back extracted with an equal volume of water; aqueous layers were combined. Samples were precipitated with ethanol three times as described above to remove the phenol, and after the last precipitation, pellets were suspended in high-performance liquid chromatography-grade water (Fisher Scientific) and lyophilized overnight in a VirTis (Gardiner, NY) BenchTop 2K lyophilizer.

PAF and PAFRa. PAF was purchased from Sigma-Aldrich. The reagent was reconstituted in ethanol and used in the experiment at a concentration of 200 nmol/l or as described in the figures. PAF was added to the transfection mixture at the apical surface as well as to the basolateral media. PAFRa (WEB 2086) was purchased from Sigma-Aldrich. The reagent was reconstituted in DMSO and used at a concentration of 1 or 10 µmol/l, added directly to the apical surface and the media 2 hours prior to transfection. The reagent was incubated with the cells throughout the transfection period.

Small molecules. All the small molecules tested were purchased from Sigma-Aldrich. The chemicals were reconstituted in appropriate solutions as recommended by the manufacturer. The epithelia were pre-treated with drugs for 6 hours at concentrations used in the CMAP study³⁰ or noted in the published literature. Following drug treatment, the epithelia were transduced with DsiRNA as described above.

Cytotoxicity assay. The LDH-cytotoxicity colorimetric assay kit (BioVision, Milpitas, CA) was used according to the manufacturer's instructions. Experimental and control samples were assayed in triplicate. The samples consisted of HAE cells treated with PAF and transduced with negative control DsiRNA or *HPRT* DsiRNA. A negative control consisted of culture medium from cells treated with DsiRNA but not PAF. The positive control medium came from cells exposed to Triton x-100 (1%) both apically and basolaterally for 30 minutes at 37 °C. After the treatment period, 100 µl of culture media was transferred into an optically clear 96-well plate and an equal volume of reaction mixture added to each well and incubated for up to 30 minutes at room temperature. The absorbance was measured at 495 nm using a microplate reader (VERSAmax, Molecular Devices, Sunnyvale, CA). The background value was subtracted and the percentage cytotoxicity was calculated using the formula: (Test sample-Negative control)/(Positive control-Negative control) × 100.

Transduction. For well-differentiated airway epithelia, transduction was performed mostly according to the manufacturer's protocol. In all cases, the apical surface of epithelia was rinsed twice with PBS before adding the transfection mixture to the apical surface. DsiRNAs were used at a concentration of 250 nmol/l. The mixture was left on the cells for 4 hours after which the medium was removed, the apical surface rinsed with PBS and the cells incubated further for 24 hours. For all experiments, a minimum of 3 biological replicates, in triplicate, were done.

RNA isolation and quantitative reverse transcription-q-PCR (RT-qPCR). Total RNA was isolated using SV96 RNA isolation kit (Promega, Madison, WI), according to manufacturer's protocol. Total RNA (250 ng) were reverse transcribed using oligo (dT) (Roche Biochemicals, Indianapolis, IN) and random hexamers (Life Technologies, Carlsbad, CA) and Superscript II (Life Technologies, Carlsbad, CA) according to manufacturer's instructions. One-fifteenth of the cDNA was then amplified and analyzed by using the 5'-nuclease assay in a 7900 Real Time PCR System (Applied Biosystems, Foster city, CA) using primer-probe pairs reaction buffer and Immolase DNA polymerase (Bioline, Taunton, MA). The sequence of the primers and probes used in the reactions are detailed in **Supplementary Table S3**. The reaction mix was contained in a total volume of 10 µl and the reaction condition was an initial cycle of 95 °C for 10 min, then 40 cycles of 95 °C for 15 s and 60 °C for 1 min. All data were normalized to the internal standard, RPL4 mRNA for pig airway samples and SFRS9 mRNA for human airway samples. Absolute quantification of an mRNA target sequence within an unknown sample was determined by reference to a standard curve. PCR efficiency for all reactions was within the acceptable margin of 90–110%. All results of the samples were presented as remaining target mRNA level in comparison to the mRNA level in the control samples (transduced with the NC1DsiRNA), which were normalized to 100%.

Connectivity map analysis. The Connectivity map (CMAP) is a public database of human cell line gene expression data sets representing responses to drug treatments that can be queried using input gene expression signatures to identify small molecules that share similar gene expression patterns.³⁰ We used input query signatures derived from published microarray data of gene expression changes associated with stimulation of PAFR.³¹ Specifically, genes with more than 3-fold expression change from 0 to 4 days culture or 0 to 8 days were used as input signatures (probe ID defined by the Affymetrix GeneChip Human Genome U133A array). Each reference signature in the database was compared with the input signature and given a score termed the "connectivity score" based on the extent of similarity between the two. Scores ranged from +1 (+ correlation), 0 (no correlation) and -1 (reverse correlation). We selected candidate agents with connectivity scores approximating +1.

RSV. For infections, RSV aliquots were resuspended in cold DMEM or DMEM/F12. RSV strain A2 (wt RSV) was kindly provided by Barney Graham (NIH, Bethesda, MD), and working stocks of RSV were prepared in HEp-2 cells (ATCC).

RSV infection. RSV infection of HAE for both for immunoblot and viral titer was done at an MOI of 1. The virus was thawed at 37 °C and diluted in MEM (0% FCS) to a volume of 70 μ l (1MOI)/well. The cells in Millicell filters were rinsed with the same media once and the virus applied to the apical surface. The plate was incubated at 37 °C for a period of 2 hours. After the incubation period, the virus inoculum was rinsed with MEM three times to remove any traces of the virus. The plates were then incubated at 37 °C until used for the assay.

Plaque assay for assessing RSV titer in cell supernatant. HEp-2 cells were seeded onto 12-well plate at a sufficient density so that it reached 90–95% confluence the next day. RSV stock was serially diluted in a 96-well u-bottom plate in serum-free MEM. 200 μ l of this dilution was added to the wells of the HEp-2 cells and allowed to incubate at 37 °C for 2 hours. At the end of the incubation period, the inoculum was removed and the cells were overlaid with 2 ml of a 1:1 mixture of complete EMEM and 1% agarose (SeaKem ME agarose, Lonza). The plates were allowed to incubate for 5 days at 37 °C. After this period, the cells were stained with a second overlay (1 ml) with a similar mixture as first, but with the addition of 0.015 % neutral red. The cells were incubated for an additional 24 hours at 37 °C after which the plaques were counted under a light box. The viral titer were then estimated as plaque forming units per ml (PFU/ml) and plotted as \log_{10} PFU/ml.

Immunoblotting. HAE were rinsed with PBS and lysed in RIPA buffer (1% NP-40, 0.5% sodium deoxycholate, 0.1% SDS, 50 mmol/l Tris, protease inhibitors [cOmplete; mini, EDTA-free; Roche Biochemicals, Indianapolis, IN]) for 30 minutes at 4 °C. The lysate were centrifuged in a table top centrifuge at 14,000 rpm for 20 minutes at 4 °C. The supernatant was quantified by BCA protein assay kit (Pierce, Rockford, IL). Thirty micrograms of protein per lane was separated on a 10% Tris-HCL Criterion precast gel (Bio-Rad, Hercules, CA) for western blot analysis. The protein was transferred to Polyvinylidene difluoride membrane and then was probed with goat anti-RSV antibody purchased from Meridian Life Sciences (Memphis, TN). The membrane was imaged, and then stripped with Restore Western Blot Stripping Buffer (Thermo Scientific, Lafayette, CO) for 15 minutes. The membrane was rinsed with Tris-buffered saline-Tween (TBS-T) and blocked in 5% bovine serum albumin (Research Products International Corp, Mt. Prospect, IL). The membrane was then re-probed with α -tubulin (Sigma-Aldrich).

Confocal imaging. The primary HAE grown at the ALI were transfected with the DIG-labeled DsiRNA at a concentration of 250 nmol/l after complexing with Transductin. The transfection mixture was left on the apical surface for 1 h. At the end of this period, the cells were fixed in 2% formaldehyde, permeabilized in 0.2 % Triton-x-100 and blocked in 1% BSA for 1 h. The cells were then stained with mouse antibody to DIG (Roche Biochemicals, Indianapolis, IN) for 1 h, followed by Alexa 488 labeled goat anti-mouse secondary antibody for 1 h, and then Alexa 488 labeled rabbit anti-mouse tertiary antibody (Life Technologies, Carlsbad, CA). In some cases an Alexa 564 goat anti-mouse secondary antibody was used. The cells were finally stained with nuclear stain, ToPro 3 for

10 minutes. The filter, containing the cells, was removed from the culture insert by cutting the edges with razor blade, and mounted on a slide with Vectashield (Vector Laboratories Inc, Burlingame, CA). The cells were visualized by confocal microscopy (Bio-Rad Radiance 2100MP Multiphoton/Confocal Microscope, Bio-Rad, Hercules, CA).

Statistical analyses. The data from quantitative experiments were analyzed using paired Student's t-test analysis or repeated measures ANOVA as appropriate. All of the data presented are representative of the results of at least three or more independent experiments.

Supplementary material

Figure S1. Dose dependency and duration of PAF-assisted DsiRNA silencing.

Figure S2. Morphology evaluation and assessment of toxicity of the PAF treatment.

Figure S3. Dose–response effect of spiperone on Transductin-DsiRNA delivery.

Figure S4. Transepithelial electrical current and conductance in HAE with different treatments.

Table S1. Description of LOS isoforms.

Table S2. DsiRNA target and sequence.

Table S3. qPCR primers and probes.

Acknowledgments. This work was supported by HL51670, DK54759, the Roy J. Carver Charitable Trust, and the University of Iowa Cystic Fibrosis Foundation RDP. The authors like to thank Phil Karp for providing the primary human airway cells, Samantha Osterhaus for helping in Ussing chamber studies and Christine Wohlford-Lenane for helping with LDH cytotoxicity assay and H&E staining. The authors also acknowledge the Central Microscopy Research Facilities for support, the Davidson and McCray labs for helpful discussions. M.A.B. is employed by Integrated DNA Technologies, Inc. which offers oligonucleotides for sale similar to some of the compounds described in the manuscript. IDT is not a publicly traded company and the author does not personally own any shares or equity in IDT.

- Sanders, N, Rudolph, C, Braeckmans, K, De Smedt, SC and Demeester, J (2009). Extracellular barriers in respiratory gene therapy. *Adv Drug Deliv Rev* **61**: 115–127.
- Zuhorn, IS, Engberts, JB and Hoekstra, D (2007). Gene delivery by cationic lipid vectors: overcoming cellular barriers. *Eur Biophys J* **36**: 349–362.
- Alvarez, R, Elbashir, S, Borland, T, Toudjarska, I, Hadwiger, P, John, M et al. (2009). RNA interference-mediated silencing of the respiratory syncytial virus nucleocapsid defines a potent antiviral strategy. *Antimicrob Agents Chemother* **53**: 3952–3962.
- Bitko, V, Musiyenko, A, Shulyayeva, O and Barik, S (2005). Inhibition of respiratory viruses by nasally administered siRNA. *Nat Med* **11**: 50–55.
- DeVincenzo, J, Lambkin-Williams, R, Wilkinson, T, Cehelsky, J, Nochur, S, Walsh, E et al. (2010). A randomized, double-blind, placebo-controlled study of an RNAi-based therapy directed against respiratory syncytial virus. *Proc Natl Acad Sci USA* **107**: 8800–8805.
- Kim, TH, Kim, SH, Seo, JY, Chung, H, Kwak, HJ, Lee, SK et al. (2011). Blockade of the Wnt/ β -catenin pathway attenuates bleomycin-induced pulmonary fibrosis. *Tohoku J Exp Med* **223**: 45–54.
- Lomas-Neira, JL, Chung, CS, Wesche, DE, Perl, M and Ayala, A (2005). *In vivo* gene silencing (with siRNA) of pulmonary expression of MIP-2 versus KC results in divergent effects on hemorrhage-induced, neutrophil-mediated septic acute lung injury. *J Leukoc Biol* **77**: 846–853.
- Merkel, OM, Zheng, M, Debus, H and Kissel, T (2012). Pulmonary gene delivery using polymeric nonviral vectors. *Bioconjug Chem* **23**: 3–20.
- Perl, M, Chung, CS, Lomas-Neira, J, Rachel, TM, Biffi, WL, Cioffi, WG et al. (2005). Silencing of Fas, but not caspase-8, in lung epithelial cells ameliorates pulmonary

- apoptosis, inflammation, and neutrophil influx after hemorrhagic shock and sepsis. *Am J Pathol* **167**: 1545–1559.
10. Rosas-Taraco, AG, Higgins, DM, Sánchez-Campillo, J, Lee, EJ, Orme, IM and González-Juarrero, M (2009). Intrapulmonary delivery of XCL1-targeting small interfering RNA in mice chronically infected with *Mycobacterium tuberculosis*. *Am J Respir Cell Mol Biol* **41**: 136–145.
 11. Senoo, T, Hattori, N, Tanimoto, T, Furonaka, M, Ishikawa, N, Fujitaka, K et al. (2010). Suppression of plasminogen activator inhibitor-1 by RNA interference attenuates pulmonary fibrosis. *Thorax* **65**: 334–340.
 12. Zhang, X, Shan, P, Jiang, D, Noble, PW, Abraham, NG, Kappas, A et al. (2004). Small interfering RNA targeting heme oxygenase-1 enhances ischemia-reperfusion-induced lung apoptosis. *J Biol Chem* **279**: 10677–10684.
 13. Ge, Q, Filip, L, Bai, A, Nguyen, T, Eisen, HN and Chen, J (2004). Inhibition of influenza virus production in virus-infected mice by RNA interference. *Proc Natl Acad Sci USA* **101**: 8676–8681.
 14. Robbins, M, Judge, A, Ambegia, E, Choi, C, Yaworski, E, Palmer, L et al. (2008). Misinterpreting the therapeutic effects of small interfering RNA caused by immune stimulation. *Hum Gene Ther* **19**: 991–999.
 15. Moschos, SA, Frick, M, Taylor, B, Turnpenney, P, Graves, H, Spink, KG et al. (2011). Uptake, efficacy, and systemic distribution of naked, inhaled short interfering RNA (siRNA) and locked nucleic acid (LNA) antisense. *Mol Ther* **19**: 2163–2168.
 16. Platz, J, Pinkenburg, O, Beisswenger, C, Püchner, A, Damm, T and Bals, R (2005). Application of small interfering RNA (siRNA) for modulation of airway epithelial gene expression. *Oligonucleotides* **15**: 132–138.
 17. Krishnamurthy, S, Behlke, MA, Ramachandran, S, Salem, AK, McCray, PB Jr and Davidson, BL (2012). Manipulation of Cell Physiology Enables Gene Silencing in Well-differentiated Airway Epithelia. *Mol Ther Nucleic Acids* **1**: e41.
 18. Ketterer, MR, Shao, JQ, Hornick, DB, Buscher, B, Bandi, VK and Apicella, MA (1999). Infection of primary human bronchial epithelial cells by *Haemophilus influenzae*: macropinocytosis as a mechanism of airway epithelial cell entry. *Infect Immun* **67**: 4161–4170.
 19. Mercer, J and Helenius, A (2009). Virus entry by macropinocytosis. *Nat Cell Biol* **11**: 510–520.
 20. Moniot, B, Declosmenil, F, Barrionuevo, F, Scherer, G, Aritake, K, Malki, S et al. (2009). The PGD2 pathway, independently of FGF9, amplifies SOX9 activity in Sertoli cells during male sexual differentiation. *Development* **136**: 1813–1821.
 21. Robbins, ML, Sekhon, RS, Meeley, R and Chopra, S (2008). A Mutator transposon insertion is associated with ectopic expression of a tandemly repeated multicopy *Myb* gene *pericarp color1* of maize. *Genetics* **178**: 1859–1874.
 22. Swords, WE, Buscher, BA, Ver Steeg li, K, Preston, A, Nichols, WA, Weiser, JN et al. (2000). Non-typeable *Haemophilus influenzae* adhere to and invade human bronchial epithelial cells via an interaction of lipooligosaccharide with the PAF receptor. *Mol Microbiol* **37**: 13–27.
 23. Cundell, DR, Gerard, NP, Gerard, C, Idanpaan-Heikkila, I and Tuomanen, EI (1995). *Streptococcus pneumoniae* anchor to activated human cells by the receptor for platelet-activating factor. *Nature* **377**: 435–438.
 24. Zhang, JR, Mostov, KE, Lamm, ME, Nanno, M, Shimida, S, Ohwaki, M et al. (2000). The polymeric immunoglobulin receptor translocates pneumococci across human nasopharyngeal epithelial cells. *Cell* **102**: 827–837.
 25. Pezzulo, AA, Starner, TD, Scheetz, TE, Traver, GL, Tilley, AE, Harvey, BG et al. (2011). The air-liquid interface and use of primary cell cultures are important to recapitulate the transcriptional profile of *in vivo* airway epithelia. *Am J Physiol Lung Cell Mol Physiol* **300**: L25–L31.
 26. Preston, A, Mandrell, RE, Gibson, BW and Apicella, MA (1996). The lipooligosaccharides of pathogenic gram-negative bacteria. *Crit Rev Microbiol* **22**: 139–180.
 27. Shukla, SD (1992). Platelet-activating factor receptor and signal transduction mechanisms. *FASEB J* **6**: 2296–2301.
 28. Knezevic, II, Predescu, SA, Neamu, RF, Gorovoy, MS, Knezevic, NM, Easington, C et al. (2009). Tiam1 and Rac1 are required for platelet-activating factor-induced endothelial junctional disassembly and increase in vascular permeability. *J Biol Chem* **284**: 5381–5394.
 29. Xu, LF, Xu, C, Mao, ZQ, Teng, X, Ma, L and Sun, M (2011). Disruption of the F-actin cytoskeleton and monolayer barrier integrity induced by PAF and the protective effect of ITF on intestinal epithelium. *Arch Pharm Res* **34**: 245–251.
 30. Lamb, J, Crawford, ED, Peck, D, Modell, JW, Blat, IC, Wrobel, MJ et al. (2006). The Connectivity Map: using gene-expression signatures to connect small molecules, genes, and disease. *Science* **313**: 1929–1935.
 31. Travers, JB, Edenberg, HJ, Zhang, Q, Al-Hassani, M, Yi, Q, Baskaran, S et al. (2008). Augmentation of UVB radiation-mediated early gene expression by the epidermal platelet-activating factor receptor. *J Invest Dermatol* **128**: 455–460.
 32. Liang, L, MacDonald, K, Schwiebert, EM, Zeitlin, PL and Guggino, WB (2009). Spiperone, identified through compound screening, activates calcium-dependent chloride secretion in the airway. *Am J Physiol Cell Physiol* **296**: C131–C141.
 33. Watts, C and Marsh, M (1992). Endocytosis: what goes in and how? *J Cell Sci* **103**: 1–8.
 34. Francis, CL, Ryan, TA, Jones, BD, Smith, SJ and Falkow, S (1993). Ruffles induced by *Salmonella* and other stimuli direct macropinocytosis of bacteria. *Nature* **364**: 639–642.
 35. Watarai, M, Derre, I, Kirby, J, Gowney, JD, Dietrich, WF and Isberg, RR (2001). *Legionella pneumophila* is internalized by a macropinocytotic uptake pathway controlled by the *Dot/lcm* system and the mouse *Lgn1* locus. *J Exp Med* **194**: 1081–1096.
 36. Imamura, J, Suzuki, Y, Gonda, K, Roy, CN, Gatanaga, H, Ohuchi, N et al. (2011). Single particle tracking confirms that multivalent Tat protein transduction domain-induced heparan sulfate proteoglycan cross-linkage activates Rac1 for internalization. *J Biol Chem* **286**: 10581–10592.
 37. Kaplan, IM, Wadia, JS and Dowdy, SF (2005). Cationic TAT peptide transduction domain enters cells by macropinocytosis. *J Control Release* **102**: 247–253.
 38. Goel, G, Makkar, HP, Francis, G and Becker, K (2007). Phorbol esters: structure, biological activity, and toxicity in animals. *Int J Toxicol* **26**: 279–288.
 39. Bussolino, F, Camussi, G, Aglietta, M, Braquet, P, Bosia, A, Pescarmona, G et al. (1987). Human endothelial cells are target for platelet-activating factor. I. Platelet-activating factor induces changes in cytoskeleton structures. *J Immunol* **139**: 2439–2446.
 40. Chao, W and Olson, MS (1993). Platelet-activating factor: receptors and signal transduction. *Biochem J* **292** (Pt 3): 617–629.
 41. Henson, PM, Barnes, PJ and Banks-Schlegel, SP (1992). NHLBI workshop summary. Platelet-activating factor: role in pulmonary injury and dysfunction and blood abnormalities. *Am Rev Respir Dis* **145**: 726–731.
 42. Shirasaki, H, Nishikawa, M, Adcock, IM, Mak, JC, Sakamoto, T, Shimizu, T et al. (1994). Expression of platelet-activating factor receptor mRNA in human and guinea pig lung. *Am J Respir Cell Mol Biol* **10**: 533–537.
 43. Stoll, LL, Denning, GM, Kasner, NA and Hunninghake, GW (1994). Platelet-activating factor may stimulate both receptor-dependent and receptor-independent increases in [Ca²⁺]_i in human airway epithelial cells. *J Biol Chem* **269**: 4254–4259.
 44. Yamaya, M, Finkbeiner, WE, Chun, SY and Widdicombe, JH (1992). Differentiated structure and function of cultures from human tracheal epithelium. *Am J Physiol* **262**(6 Pt 1): L713–L724.
 45. Amarzguoui, M, Lundberg, P, Cantin, E, Hagstrom, J, Behlke, MA and Rossi, JJ (2006). Rational design and *in vitro* and *in vivo* delivery of Dicer substrate siRNA. *Nat Protoc* **1**: 508–517.
 46. Collingwood, MA, Rose, SD, Huang, L, Hillier, C, Amarzguoui, M, Wiiger, MT et al. (2008). Chemical modification patterns compatible with high potency dicer-substrate small interfering RNAs. *Oligonucleotides* **18**: 187–200.
 47. Eguchi, A, Meade, BR, Chang, YC, Fredrickson, CT, Willert, K, Puri, N et al. (2009). Efficient siRNA delivery into primary cells by a peptide transduction domain-dsRNA binding domain fusion protein. *Nat Biotechnol* **27**: 567–571.
 48. Lee, NG, Sunshine, MG, Engstrom, JJ, Gibson, BW and Apicella, MA (1995). Mutation of the *htrB* locus of *Haemophilus influenzae* nontypable strain 2019 is associated with modifications of lipid A and phosphorylation of the lipo-oligosaccharide. *J Biol Chem* **270**: 27151–27159.
 49. McLendon, MK, Schilling, B, Hunt, JR, Apicella, MA and Gibson, BW (2007). Identification of LpxL, a late acyltransferase of *Francisella tularensis*. *Infect Immun* **75**: 5518–5531.



This work is licensed under a Creative Commons Attribution-NonCommercial-NoDerivs 3.0 Unported License. The images or other third party material in this article are included in the article's Creative Commons license, unless indicated otherwise in the credit line; if the material is not included under the Creative Commons license, users will need to obtain permission from the license holder to reproduce the material. To view a copy of this license, visit <http://creativecommons.org/licenses/by-nc-nd/3.0/>

Supplementary Information accompanies this paper on the Molecular Therapy–Nucleic Acids website (<http://www.nature.com/mtna>)